

# Stacking fault energy and planar defects on the basal plane in the beta-alumina system

R. STEVENS, L. J. MILES

*Materials Science Section, The Electricity Council Research Centre, Capenhurst, Chester, UK*

Commercial forms of beta alumina have been examined using transmission electron microscopy. Measurements of the stacking fault energy on the basal plane have been made from the separation of partial dislocations and the equilibrium separation of partials at dislocation nodes, and estimated as  $0.6$  to  $1.65 \times 10^{-3} \text{ J m}^{-2}$ . The structure of two- and three-block beta-alumina has been discussed and their relationship and transformation examined. It has been shown that transformation from two- to three-block beta-alumina cannot be accomplished by a simple shear. Structures generated by the passage of partial dislocations on the glide plane are discussed, and simple twinning on the basal plane is examined and shown to be possible in the three-block, but not in the two-block material.

## 1. Introduction

Beta-alumina is the name used to describe a series of complex sodium aluminates. These are characterized by possession of appreciable ionic conductivity at relatively low temperatures and this makes them suitable for use as electrolyte in electrochemical devices [1]. Physical and chemical properties are improved by the addition of other oxides such as lithia and magnesia [2, 3].

The stoichiometric compound of beta-alumina,  $\text{Na}_2\text{O} \cdot 11\text{Al}_2\text{O}_3$ , has a hexagonal crystal structure  $P6_3/mmc$ . The unit cell has been described [4, 5] and consists of blocks of four layers of close packed oxygen ions with the aluminium ions distributed similarly to the cations in common spinel  $\text{MgO} \cdot \text{Al}_2\text{O}_3$ . Between each "spinel" block is a relatively sparsely populated plane containing all the sodium ions and oxygen ion "bridges". The "spinel" blocks on either side of the sodium-rich interconnecting layer are mirror images of each other and the unit cell has dimensions  $a_0 = 0.559 \text{ nm}$  and  $C_0 = 2.26 \text{ nm}$ .

In practice, there is always an excess of soda over that required by stoichiometry and this is compensated either by aluminium ion vacancies or substitution for aluminium with an ion of lower valency so as to maintain charge neutrality.

Phases with higher soda contents than

$\text{Na}_2\text{O} \cdot 11\text{Al}_2\text{O}_3$  have been reported. Earlier researchers have discovered the compounds  $\text{Na}_2\text{O} \cdot 0.8\text{Al}_2\text{O}_3$  [5],  $\text{Na}_2\text{O} \cdot 0.6\text{Al}_2\text{O}_3$  [6] and  $\text{Na}_2\text{O} \cdot 0.5\text{Al}_2\text{O}_3$  [7], as well as structures where the spinel blocks contain six layers of oxygen ions [8]. The more important of these compounds,  $\text{Na}_2\text{O} \cdot 0.5\text{Al}_2\text{O}_3$  has been called  $\beta''$  alumina and the crystal symmetry belongs to the rhombohedral space group  $R3m$ . The unit cell is composed of three spinel blocks connected by two soda-rich layers. Unlike  $\beta$  alumina there is no mirror symmetry across these layers which, therefore, can be classed as glide planes. The dimensions of the unit cell are  $a_0 = 0.561 \text{ nm}$  and  $C_0 = 3.39 \text{ nm}$ . The stoichiometric formula corresponds to two sodium ions per unit cell, charge compensated by aluminium ion vacancies. The structure determined in this manner is unstable and so  $\text{MgO}$  or  $\text{Li}_2\text{O}$  is usually added as a stabilizer. In practice, less than the stoichiometric amount of soda is present so that the structure may be regarded as containing defects in the conducting plane. Owing to the relative shift of the spinel blocks in the glide plane both sodium ions reside in identical sites and are also able to diffuse more easily through the plane. The structure has been developed and discussed in detail by Bettman and Peters [9, 10].

Beta-alumina used as solid electrolyte in tech-

nological applications often consists of mixtures of the two phases, “two-block”  $\beta$  and “three-block”  $\beta''$ . The proportions of each is determined by firing schedules and chemical composition and so the fine structure of many types of material is expected to be complex.

## 2. Experimental techniques

Beta alumina, both sintered and hot pressed, was obtained from a number of sources, usually commercial research laboratories. Single crystal  $\beta$  alumina was obtained from a brick of fusion cast Monofrax, a refractory used as a liner in glass melting furnaces, nominally  $\text{Na}_2\text{O} \cdot 11\text{Al}_2\text{O}_3$ , but usually containing an excess of soda.

Thin ( $\sim 1$  mm) sections of ceramic were cut from the samples and supported on a glass microscope slide using thermosetting Lakeside resin. Chips of single crystal were mounted in a similar fashion. The ceramic was then polished flat through a series of silicon carbide papers, and finally finished on  $4\ \mu\text{m}$  diamond powder. The polished surfaces were reversed on the glass slide and the operation repeated until the ceramic sections were 25 to  $50\ \mu\text{m}$  thick. Areas 2 to  $4\ \text{mm}^2$  were then removed, cleaned and mounted on 3 mm diameter copper supports, having a 1 mm diameter central hole. Final thinning was carried out on an Edwards ion-beam thinning device, an angle of attack of 15 to  $20^\circ$ , a voltage of 6 to 7 kV and a current of 50 mA being used. This allowed thinning rates of  $0.5\ \mu\text{m h}^{-1}$  and a 75% success rate in obtaining suitably thin foils.

The thin foils of beta alumina were examined in a Phillips EM200 electron microscope at 100 kV, using a goniometer stage having  $\pm 30^\circ$  tilt on two perpendicular axes. The instrument was also equipped with electromagnetic beam tilting facilities.

## 3. Stacking fault energy

Measurement of stacking fault energy using transmission electron microscopy is a well established technique and can be achieved by several [11]. The original investigation, using the measurement of extended dislocation nodes, equated the line tension of the dislocation partials with the area of stacking fault under equilibrium conditions. The theoretical analysis has been refined several times since, an account being given in the review by Ruff [12]. A similar technique utilizes the equilibrium separation of partial dis-

locations generated from an isolated unit dislocation [13]. Both techniques can be applied only to low stacking fault energy materials using isolated dislocations, although they have found wide application as a method of standardizing techniques used on higher stacking fault energy materials.

Successful measurements have also been made on multiple ribbon strands, extended and fault dislocation dipoles and stacking fault tetrachedra.

In beta-alumina the unit dislocation lying in the basal plane may dissociate into two or four partials resulting in the formation of one or three stacking faults accordingly [14]:

$$\frac{a}{3}\langle 11\bar{2}0 \rangle \rightarrow \frac{a}{6}\langle 11\bar{2}0 \rangle + \frac{a}{6}\langle 11\bar{2}0 \rangle \quad (1)$$

$$\frac{a}{3}\langle 11\bar{2}0 \rangle \rightarrow \frac{a}{6}\langle 1\bar{1}00 \rangle + \frac{a}{6}\langle 0\bar{1}10 \rangle + \frac{a}{6}\langle 1\bar{1}00 \rangle + \frac{a}{6}\langle 0\bar{1}10 \rangle. \quad (2)$$

Dislocations dissociation has been predicted and the stacking faults analysed and observed for splitting into four partials in chromium chloride and chromium bromide [15], and also in the case of talc, a layer type structure [16]. A summary of this work has been made by Amelinckx [17].

The stacking fault energy of  $\beta$ -alumina may be estimated from the formula:

$$\gamma = \frac{0.3Gb^2}{W} \quad (3)$$

where  $\gamma$  is the stacking fault energy,  $G$  is the shear modulus,  $b$  is the Burgers vector and  $W$  is the width of the node [11]. An hexagonal network containing extended nodes is shown in Fig. 1.

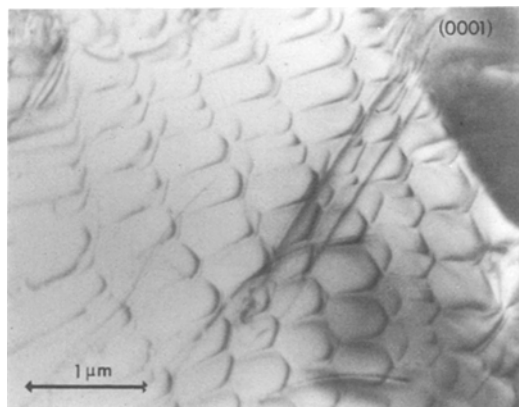


Figure 1 Hexagonal dislocation network in single crystal monofrax showing equilibrium nodes.

Such networks are rarely seen and when they occur it is usually in a fairly thick section of the foil. Difficulty is encountered in obtaining accurate measurements, since the specimen charges in the electron beam, resulting in an instability and thus a poor quality electronmicrograph. Electrostatic effects may be minimized by working as rapidly as possible, this, however, excludes extensive tilting and photographic work.

From Fig. 1 the node width  $W \approx 45$  nm. A value of the shear modulus  $G$  may be obtained from  $E = 1.6 \times 10^{11}$  N m<sup>-2</sup> by using

$$G = \frac{E}{2(1-\nu)},$$

which assuming Poissons ratio  $\nu = 0.33$  gives  $G = 10^{10}$  N m<sup>-2</sup>. The Burgers vector  $\mathbf{b} = a/6 [1\bar{1}00] = 0.16$  nm, i.e. the value for one of the four partials, yielding an estimate for the stacking fault energy  $\gamma = 1.65 \times 10^{-3}$  J m<sup>-2</sup>. The stacking fault energy of faults on the basal plane is thus low for an oxide material and is of the same order as that measured for layered ceramic materials such as graphite [17]. The calculated value should only be regarded as approximate in that no account is taken of the anisotropy of the elastic constants which can have a strong influence on the result. At present there are no data available on elastic constants in different crystallographic directions for beta alumina, the only measurement having been limited to polycrystalline material.

An alternative method of measuring stacking fault energy is by determination of the equilibrium separation  $d$  of two partial dislocations having Burgers vectors  $\mathbf{b}_1$  and  $\mathbf{b}_2$  in a long extended dislocation. In Fig. 2 several dislocations can be seen to have split up into four partial dislocations and it is reasonable to suppose that they have the Burgers vectors of the type given by Equation 2, since the dislocations are extended along the basal planes. The stacking fault energy  $\gamma$  is given by [11]:

$$\gamma = \frac{G\mathbf{b}_1\mathbf{b}_2}{8\pi d} \left( \frac{2-\nu}{1-\nu} \right) \left( 1 - \frac{2\nu \cos 2\alpha}{2-\nu} \right) \quad (4)$$

where  $G$  is the shear modulus,  $\nu$  is Poissons ratio and  $\alpha$  is the angle between the dislocation line and the total Burgers vector of the dislocation. Using a measured value of  $d \approx 300$  nm (Fig. 2),  $\alpha = 60^\circ$  and  $\mathbf{b}_1 = a/6 (1\bar{1}00)$ ,  $\mathbf{b}_2 = a/6 (0\bar{1}10)$ , and assuming  $\nu = 0.33$ , a value of  $\gamma = 6 \times 10^{-4}$  J m<sup>-2</sup> is

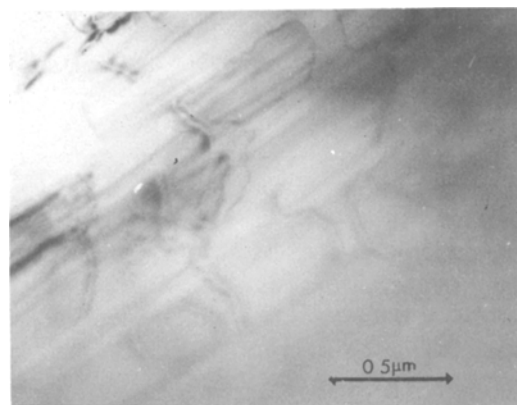


Figure 2 Separation of partial dislocations in the basal plane of beta-alumina. Note the uniform separation of the first and second partials and the third and fourth partials.

obtained which is in good agreement with the node measurements, considering the approximations and practical constraints of the method [12].

It is noticeable that this last result applies to the stacking fault generated between the first and second partial dislocations or the third and fourth partial dislocations. In the micrograph (Fig. 2) it can be seen that the distance between these partials is fairly constant, whereas the separation of the second and third partials is larger and varied, indicating the different nature of the stacking fault and the lower stacking fault energy of the fault between the second and third partials. The use of Equation 4 can be justified since the region between the second and third partials does not have a stacking fault in the oxygen ion sequence, as will be shown later.

#### 4. $\beta - \beta''$ relationships and polytypes

Although the stacking fault energy of beta alumina is low, it will be shown later that the transformation of  $\beta$  to  $\beta''$  by a shear mechanism requires rearrangement in the spinel block and thus only defect structures can be readily introduced. However, both  $\beta$  and  $\beta''$  phases may exist as separate grains or be coincident in a single grain of the same polycrystalline body. Diffraction patterns of  $\beta$  and mixed crystals are shown in Fig. 3 and 4, together with the diagrammatic pattern. Single phase  $\beta''$  could not be used in this investigation since it is difficult to manufacture reproducibly. An analysis of the beta-alumina diffraction patterns has been carried out and the  $10\bar{1}0$  pattern presents the

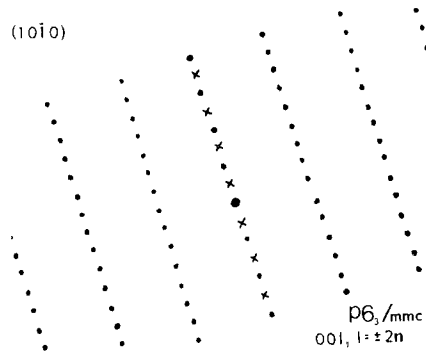
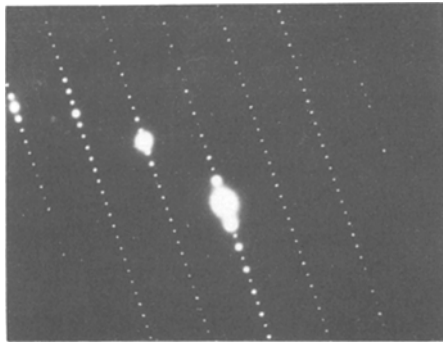


Figure 3 Diffraction pattern  $(10\bar{1}0)$  of two-block beta-alumina together with the diagrammatic pattern.

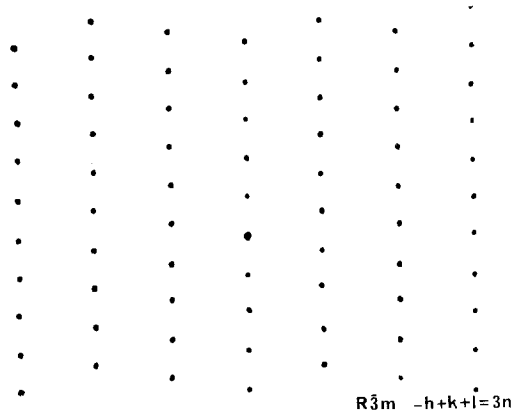
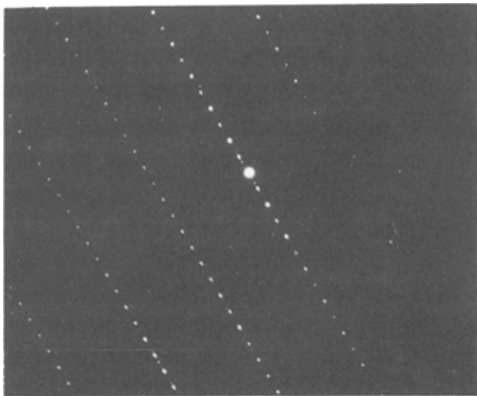


Figure 4 Diffraction pattern of mixed,  $\beta$  and three-block  $\beta''$ -alumina together with the diagrammatic pattern for  $\beta''$ .

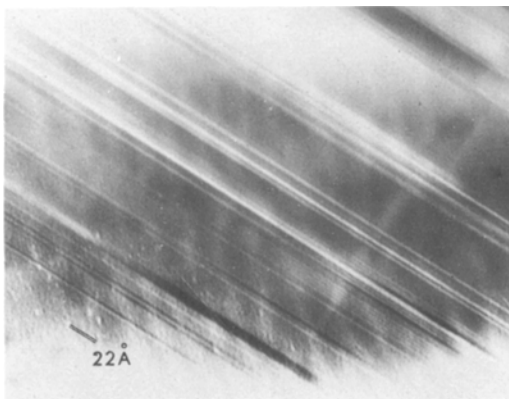


Figure 5 Resolution of the 22 Å spacing in two-block crystals. Larger spacings are also visible in the same area of foil.

easiest method of determining which phase is present in the crystals. Lattice planes may then be resolved in  $(10\bar{1}0)$  sections of the sample by the standard interference method. To obtain the results shown in Fig. 5 which is of two-block  $\beta$

giving a spacing of 2.2 nm and Fig. 6 of three-block  $\beta''$  giving 3.3 nm, the beam tilting facilities were employed to produce an image by the interference of diffracted beams with the transmitted beams. The tilting facilities allow both types of beams to lie along the axis of the microscope, maintaining resolution. A detailed description of the technique has been given elsewhere [18]. Apart from the 2.2 and 3.3 nm spacings multiples of these spacings are also readily visible.

The crystallographic relationship of the phases is such that both the basal planes and primary crystallographic directions are parallel. Since the crystallography of the phases is similar in two directions and only varies in the third, i.e. in the manner in which the blocks or spinel layers are stacked, then the two forms  $\beta$  and  $\beta''$ , might be considered to be polytypes [19], rather than distinct phases. Further weight is added to this view by the fact that both  $\beta$  and  $\beta''$  exist in the same polycrystalline body of a nominally single chemi-



Figure 6 33 Å spacing typical of the three-block  $\beta''$  structure.

cal composition. As is shown by the measurement of stacking fault energy, the energy difference between a sheared and unsheared region in the basal glide plane is very small. Dislocation motion and thus shear can readily occur [14], causing relative atomic movements on the glide plane akin to the  $\beta/\beta''$  transformation. The  $\beta/\beta''$  transformation can be produced by increasing the sodium content and by additions of MgO and Li<sub>2</sub>O [20]. The MgO and Li<sub>2</sub>O are thought to stabilize the structure when additional sodium atoms are introduced into the conducting plane by allowing the necessary ionic charge balance.

The clearest picture of the relationship of the crystallographic forms may be seen by examination of a diagrammatic ball model of the oxygen ions. Fig. 7a shows the (11 $\bar{2}$ 0) plane of close-packed spheres of the hexagonal two-block structure. It can be seen that the top spinel block has undergone a rotation of  $\pi$  with respect to the lower, and that the conducting plane is a mirror plane. If each layer of the close packed oxygen ions is designated. A, B, C then the mirror symmetry of the lattice is made obvious. A similar model is shown in Fig. 7b for the three-block structure.

The Burgers vector of dislocations and the slip system in the two block  $\beta$  has been predicted and observed [14]. In  $\beta''$  alumina, since the sodium containing plane exhibits the same periodicity, identical dislocations can be expected, i.e. two or four partial dislocations with a single or treble fault between them. Partial dislocations have been observed in crystals of mixed structures. In Fig. 8,

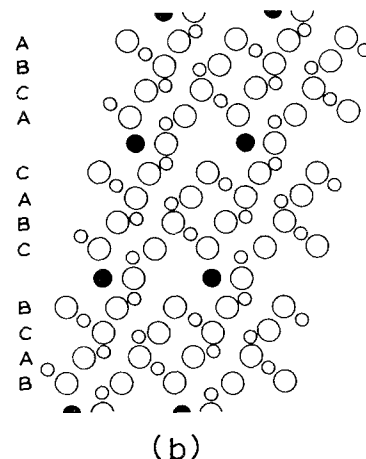
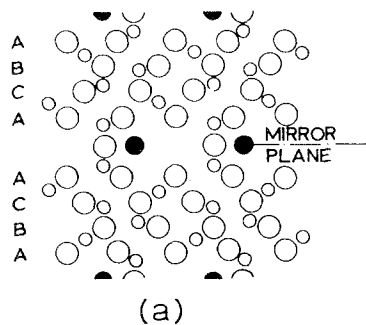


Figure 7 Ball model of the hexagonal two-block  $\beta$  structure (a), and the three-block  $\beta''$  structure (b), based on the positions of the oxygen ions in the lattice. The section shows a (11 $\bar{2}$ 0) plane. The letters A, B, C, denote the stacking position of the close-packed planes of oxygen ions in the spinel structure.

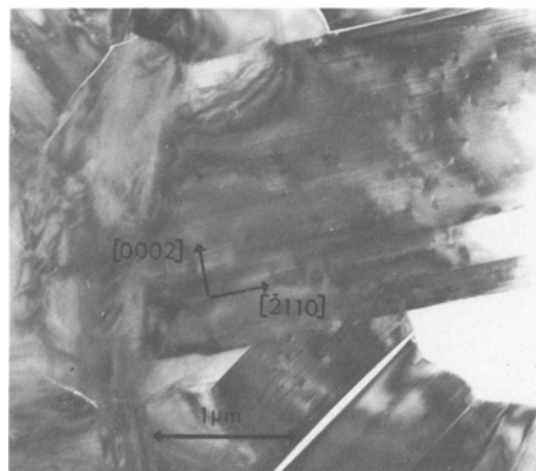


Figure 8 Dislocations viewed parallel to the electron beam. The ends of the dislocations show the characteristic light and dark contrast where they emerge from the foil.

dislocations can be seen "end on" exhibiting the characteristic light and dark contrast at the dislocation surface intersection. A "trace" of each dislocation is also visible along the projection of the basal plane onto the foil surface. It is evident that passage of the dislocation disturbs the relative structure above and below the sodium-containing plane, and hence the stacking sequence in the  $C_0$  direction.

To allow the A, B, C stacking sequences of the oxygen ions to be illustrated, a section through the  $(11\bar{2}0)$  plane is taken. In all the relative movements of each layer the partial dislocations are parts of a unit dislocation which lie in the basal plane and move in a close-packed direction, i.e.  $(11\bar{2}0)$ . The relative movements of stacking sequence must, therefore, be projected onto the  $(11\bar{2}0)$  plane to avoid possible confusion of A and C layer positions.

If one considers the stacking sequence of each of the close-packed oxygen planes in the spinel block and designate each plane A, B and C, then the stacking sequence of the unit cell (Fig. 7a) becomes for the two-block structure:



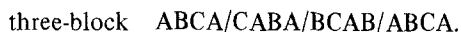
Passage of a partial dislocation  $a/6 [1\bar{1}00]$  causes the sequence to change to:



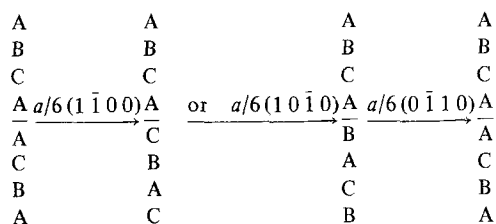
and the original structure is restored on passage of a further  $a/6 [1\bar{1}00]$  dislocation. This is significant in that stacking faults in the oxygen ion layers only exist between the first and second partial dislocation and the third and fourth. A stacking fault does exist between the second and third partial dislocations due to the rearrangement of the aluminium ions.

The region between the second and third dislocation consists of a perfect arrangement of oxygen ion layers with an adjacent "dangling bond" of the partial dislocation [21]. It is not possible for dislocations on the mirror or sodium containing plane to transform the two-block  $\beta$  to three-block  $\beta''$ . For the transformation to occur the stacking sequence in the spinel blocks themselves must be rearranged; the actual stacking sequence and structure is shown in Fig. 7b, for the three-block  $\beta''$ . For the two-block to transform to three-block

rearrangement of the stacking sequence must occur:



As can be seen when the stacking sequences are directly compared, two rearrangements in the stacking sequence in the second and one in the third spinel block are necessary to transform the three-block  $\beta''$  to two-block  $\beta$ . This movement is not possible with partial dislocations on the glide plane alone. For the two-block  $\beta$ :



The three-block  $\beta''$  should have the stacking sequence (Fig. 7b) ABCA/CABC/BCAB. It can be seen that the second two layers of the second spinel block are not the same and are in fact inverted, when compared with layers in the two-block that have undergone shear. Such a situation may be remedied by a shear within the spinel block allowing a complete transformation.

The passage of partial dislocations on the sodium-containing plane allows the generation of numerous and varied stacking faults in the  $C_0$  direction. The presence of such stacking faults in either structure would manifest itself in the streaking of the diffraction spots, in this case in the  $000n$  direction and is seen in a  $(10\bar{1}0)$  diffraction pattern.

If stacking faults are introduced by partial dislocations at regular intervals, it can produce new structures. If one considers the oxygen ion layers we have:



Passage of a single partial  $a/6 (10\bar{1}0)$  gives:

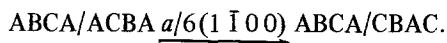
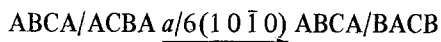


and a second partial  $a/6 (0\bar{1}10)$  produces:



i.e. the original structure once again. It is, therefore, possible to have a complex periodic

layer structure generated by the passage of partial dislocations at regular intervals. In addition, different partial dislocations of the same set will generate slightly different structures:



Thus any suitable combination of these sub-blocks may give rise to long sequence stacking arrangements. For example a partial dislocation every third spinel layer could give rise to a unit of:



More complicated structures may be produced by the introduction of partial dislocations at greater distances or at two or more different, but regular sequences, giving rise to complicated polytypes as in the case of SiC [22]. It should be apparent that similar behaviour could be expected in the three-block  $\beta''$  structure.

An important consequence of the stacking arrangements whether regular or otherwise is the explanation of multiple separation lattice fringe spacings observed in thin sections of  $\beta$ -alumina using transmission electron microscopy. In the case illustrated above, the spacing would differ from the original 2.2 nm and there is a possibility of 1.1 nm spacings and multiples thereof. Thus the original two-block structure modified by the passage of partial dislocations could be confused with the three-block structure which has an intrinsic spacing of 3.3 nm. Virtually all the low multiples of the lattice spacings have been observed [23], often in the same area of transmission foil.

It is known that partial dislocations are readily mobile in  $\beta$ -alumina [14] and their movement can thus account for the multiplicity of fringe spacings. It should be emphasized, however, that the partial dislocations generating fringe spacings in the two-block and three-block cannot transform two-block to three-block and vice versa.

## 5. Basal twinning

Twinning can occur mechanically by shear mechanisms or thermally as when growth twins develop. Deformation takes place by the passage of partial dislocations in the mirror plane of two block beta alumina. Passage of a partial dislocation  $a/6$

$[1\bar{1}00]$  gives a structure



A shear structure is developed rather than a twin, since no mirror symmetry exists across the sheared region. Should the fault be produced at regular intervals then a new layer structure is evident.



If the two-block system is designated 2H [19] then the structure is a 6R variant, produced by movement of a partial dislocation on every second mirror plane.

During growth, it is possible that different stacking sequences of oxygen ion layers may occur and one of these is equivalent to a  $\pi$  rotation of a spinel block about the "a" axis. This gives the structure:



The middle spinel block is only compatible with the two-block structure on one side due to lack of mirror symmetry at the faulted region. When the fault is produced regularly every third spinel block, a new simple layer structure is produced which can be designated 6H.



The higher order "H" polytypes can be generated by having the fault at a greater separation but still occurring in a regular sequence.

Similar reasoning may be applied to the three-block system. The original stacking sequence of the oxygen ions in the spinel blocks is:



Passage of a simple partial dislocation can produce



so that twinning cannot be produced by shear on the glide plane. As with two-block, further structures can be produced by shear at regular intervals leading to more complex polytypes.

Twinning in the three-block can occur by the inversion ( $\pi$ rotation about "a" axis) of three spinel

blocks as is shown in the following sequence:

3-block ABCA/CABC/BCAB/ABCA/CABC/BCAB/ABCA . . .

3-block ABCA/CABC/BCAB//BACB/CBAC/ACBA//ABCA . . .

$\pi$  rotation

2-block BCAB//BACB ACBA//ABCA.

The structure developed is twinned and has structural features similar to 6H obtained from a  $\pi$  rotation in two-block. It differs in that at the non-faulted planes, the structure has the three-block crystal symmetry whereas at the mirror planes two-block symmetry exists. This structure may thus be regarded as a mixed  $\beta/\beta''$  crystal.

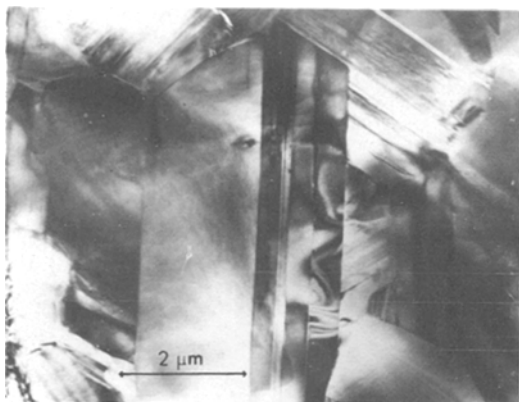


Figure 9 Twinning in commercial beta-alumina. The twin axis is parallel to the length of the grain.

Basal twinning is often observed in polycrystalline  $\beta/\beta''$  alumina material developed for electrolyte applications. The electron micrograph Fig. 9, shows a twin in this material extending the length of the grain, the major axis of the twin lying along a projection of the basal plane. As was shown earlier they can only be formed by a growth mechanism and not by shear along glide planes. Such twins are nearly always present in recrystallized material where grain growth has occurred. In this particular case individual grains are made up of lamellae of twins and are clearly visible as

in the electron micrograph (Fig. 9) where one half of the grain can be seen to be built of successive layers of twins.

## References

1. N. WEBER and J. T. KUMMER, *Intersoc. Energ. Convers. Engng. Conf.* (1967) p. 913.
2. Annual Report, Ford Motor Company, NSF Contract C805, (June 1974).
3. I. WYNN JONES and L. J. MILES, *Proc Brit. Ceram. Soc.* **19** (1971) 161.
4. C. A. BEEVERS and M. A. S. ROSS, *Z. Krist* **97** (1937) 59.
5. G. YAMAGUCHI and K. SUZUKI, *Bull. Chem. Soc. Japan* **41** (1968) 93.
6. R. SCHOLDER and M. MANSMANN, *Z. Anorg Allgem. Chem.* **321** (1963) 246
7. J. THERY and D. BRIANCON, *Rev. Hautes Temp. Refract* **1** (1964) 221.
8. M. BETTMAN and L. L. TERNER, *Inorg Chem.* **10** (7) (1971) 1442.
9. M. BETTMAN and C. R. PETERS, *J. Phys Chem* **73** (1969) 1774.
10. C. R. PETERS, M. BETTMAN, J. W. MOORE and M. D. GLICK, *Acta. Cryst.* **B27** (1971) 1826.
11. "Electron Microscopy of Thin Crystals", P.B. Hirsch, A. Howie, R.B. Nicholson, D.W. Pashley and M.J. Whelan (Butterworths, London, 1965).
12. A. W. RUFF, *Met. Trans.* **1** (1970) 2391.
13. S. AMELINCKX and P. DELAVIGNETTE, *J. Appl. Phys.* **31** (1960) 2126.
14. R. STEVENS, *J. Mater. Sci.* **9** (1974) 801.
15. P. DELAVIGNETTE and S. AMELINCKX, *Trans. Brit. Ceram Soc.* **62** (1963) 687.
16. S. AMELINCKX and P. DELAVIGNETTE, *J. Appl. Phys.* **32** (1961) 3, 341.
17. S. AMELINCKX, *Sol. Stat. Phys.* **6** (1964) 291.
18. V. A. PHILLIPS and J. A. HUGO, *Acta Met.* **18** (1970) 123.
19. A. J. VERMA and P. KRISHNA, "Polymorphism and Polytypism in Crystals" (Wiley, London, 1966).
20. L. J. MILES and I. WYNN JONES, Extended Abstracts, Electrolytes for Power Sources, Soc. for Electrochem., Brighton (December 1973).
21. J. HORNSTRA, *J. Phys. Chem. Solids* **5** (1958) 129.
22. P. T. B. SHEAFFER, *Acta Cryst.* **B25** (1969) 3, 477.
23. D. J. M. BEVAN, B. HUDSON and P. T. MOSELEY, *Mat. Res. Bull.* **9** (1974) 1073.

Received 26 January and accepted 26 March 1976.